ISSN 2635-1676, Nanobiotechnology Reports, 2024, Vol. 19, No. 2, pp. 275–281. © Pleiades Publishing, Ltd., 2024.

DEVICES AND PRODUCTS BASED ON NANOMATERIALS AND NANOTECHNOLOGIES

Application of ZIF-8/ZIF-67 Multilayer Films for NO_2 and CO Detection

O. I. Il'in[a,*], V. A. Polyakov[b], N. N. Rudyk[a], Yu. Yu. Zhityaeva[a], A. V. Saenko[a], M. A. Gritsai[b], A. A. Chefranov[a], and M. A. Soldatov[b]

[a] *Institute of Nanotechnologies, Electronics, and Instrumentation Technology, Southern Federal University, Taganrog, Russia*

[b] *Smart Materials Research Institute, Southern Federal University, Rostov-on-Don, Russia*

**e-mail: oiilin@sfedu.ru*

Received November 24, 2023; revised December 25, 2023; accepted December 25, 2023

Abstract—Prototypes of gas sensors with sensitive elements are made based on ZIF-8 and ZIF-67 films obtained directly on a substrate by immersion. The sensitivity of the prototypes to NO_2 and CO is assessed by simultaneously analyzing the capacitive and resistive response. It is shown that the functionalization of ZIF-8 films with layers of ZIF-67/ZIF-8 leads to an increase in the sensitivity of the sensor to NO_2 by more than 2 times compared to ZIF-8 films, and also allows CO detection. A sensor prototype based on ZIF-67/ZIF-8 films shows a resistive and capacitive sensitivity to NO_2 of 3 and 6% (for 45 ppm), 14 and 15% (for 85 ppm), and to CO of 9 and 7% (for 6 ppm), 15 and 10% (for 10 ppm). It is shown that parallel analysis of the capacitive and resistive response makes it possible to increase the accuracy of the analysis of the sensor response when exposed to various gases and can be used as the basis for a software interface for training sensor operation using artificial intelligence.

DOI: 10.1134/S2635167624600949

INTRODUCTION

With the development of technologies in the field of nanomaterials, the Internet of things and artificial intelligence (AI), the requirements for the sensitive elements of gas sensors (device dimensions, price, energy efficiency, sensitivity, and stability of characteristics [1–4]), used for monitoring air quality both indoors and outdoors, are increasing [5]. At the same time, acoustic and calorimetric gas sensors are difficult to scale, which limits their integration with components of microelectronic circuits. Chemoresistive gas sensors based on metal-oxide semiconductors or carbon nanomaterials have found wide application, but the challenges of increasing energy efficiency, sensitivity, selectivity, and stability remain open [6, 7]. Nondispersive IR (infrared) gas sensors have attractive characteristics, including high sensitivity, selectivity, reliability, and a long service life, but their high cost, design complexity, and miniaturization challenges limit their application.

In this regard, there is a gradual transition from the use of inorganic materials based on silicon and metal oxides to organic and hybrid organic-inorganic materials [8]. Such materials could offer benefits in terms of structural diversity, reduce manufacturing costs, and enable miniaturization of logic components down to the molecular scale. One of the most promising materials for such applications is metal-organic framework (**MOF**) structures [9]. MOFs consisting of metal nodes and organic linkers have an exceptionally large surface area, ultra-high porosity, and a diverse structure with short- and long-range order [10]. Therefore, MOFs open up broad opportunities for creating nanoscale energy-efficient gas sensors for stationary and wearable electronics. The first studies concerning the use of these materials as sensitive elements of gas sensors appeared less than 15 years ago [11]. However, the designs of the proposed sensor systems and signal processing were quite complex [12, 13], which limited their use for mass production [14, 15]. In this regard, the development of a technologically advanced and low-cost sensor design based on MOF, as well as a technique for detecting multiple signals, which makes it possible to improve the quality of gas recognition, is an urgent task, the solution of which will significantly increase the selectivity of operation and applicability of the sensor.

In this work, prototypes of gas sensors with sensitive elements based on films of zeolitic imidazolate frame (**ZIF**) structures ZIF-8, ZIF-8/ZIF-67 and their sensitivity to NO_2 and CO are studied with parallel analysis of the capacitive and resistive response of the sensors, making it possible to simplify and reduce the cost of their production technology.

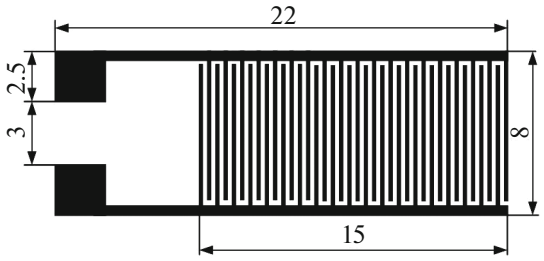

Fig. 1. Topology of the photo template of the gas-sensor prototype.

METHODS AND MATERIALS

Sensor manufacturing. In the manufacture of prototypes of gas sensors with sensitive elements based on ZIF-8 and ZIF-8/ZIF-67 films, quartz glass was used as the substrate. Using the magnetron sputtering of a chromium (99.99%, Girmet, Russia) and copper (99.99%, Girmet, Russia) target, a three-layer structure was formed based on Cr (15 nm)/Cu (100 nm)/Cr (15 nm) metal films.

The topology of the electrodes was formed by photolithography using an MJB4 installation (SUSS, Switzerland) with an FP-383 positive resist (Frast-M, Russia). The design of the photomask was developed based on interdigitated electrodes (Fig. 1). The width of the electrodes, equal to the gap between them, was 200 μm. The size of the pads for connecting the measuring equipment was 2.5×2.5 mm^2. To form the pattern of interdigitated electrodes, liquid etching of a multilayer film was carried out in based solutions: HCl : H_2O (1 : 1) for Cr and H_3PO_4 : HNO_3 : CH_3COOH : H_2O (45 : 2 : 9 : 3) for Cu.

Then, MOF films were grown based on ZIF, which is a porous zinc 2-methylimidazole with sodalite topology [16], according to a previously described method [17]. The advantage of ZIF is its high thermal stability, large specific surface area up to 2000 m^2/g, and excellent sorption properties [18]. Synthesis was carried out for 30 min; it corresponded to one cycle of film deposition. The deposition of MOF films was monitored using scanning electron microscopy (**SEM**) (Nova Nanolab 600, Netherlands) and X-ray diffraction (**XRD**) (D2 PHASER, USA). As a result, two types of sensor prototype were formed: the first (S_1) based on ZIF-8 films (Fig. 2a), the second (S_2) based on a ZIF-8/ZIF-67 multilayer film (Fig. 2b) with five deposition cycles each.

Measuring stand. Studying the influence of the target gases NO_2 and CO on the resistive and capacitive characteristics of the sensing element were carried out using an E4980A impedance meter (Agilent, USA). The choice of target gases is related to their potential danger to humans both in confined spaces and outdoors.

Measurements were carried out in the range of 20 Hz–2 MHz with simultaneous measurement of the impedance Z and phase angle θ (impedance phase). During the measurement process, statistical data was accumulated to obtain the median value of the capacitance and resistance for each point in time/frequency based on the results of 10 measurements. The voltage supplied to the sensor was 1 V.

Gas measurements were carried out in a specialized Microgas-FM installation (ZAO Intera, Russia), which allows the mixing of flows of diluent gas and target gas in parts of up to 100 : 1. Air (N_2 (80%) + O_2 (20%)) was used as the diluent gas, and as the target gases, test-gas mixtures of CO (60 ppm) and NO_2 (515 ppm) were employed. Twenty minutes after the start of purging with synthetic air, the target gas was supplied for 20 minutes, after which the supply of the target gas was stopped and purging with synthetic air continued for another 20 min.

The sensitivity of the sensor was assessed by the relative change in the resistance (S_R, for the resistive response) and capacitance (S_C, for the capacitive response):

$$S_{R,C} = \frac{X_g}{X_a} \times 100\%,$$

where X_g is the resistance (R_g) or capacity (C_g) of the sensor when exposed to a certain concentration of target gas, X_a is the resistance (R_a) or capacity (C_a) of the material in an air atmosphere.

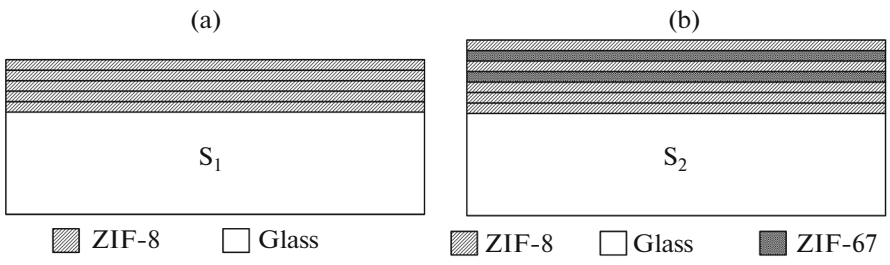

Fig. 2. Structure of a sensing element based on multilayer MOF films for sensor prototype S_1 (a) and S_2 (b).

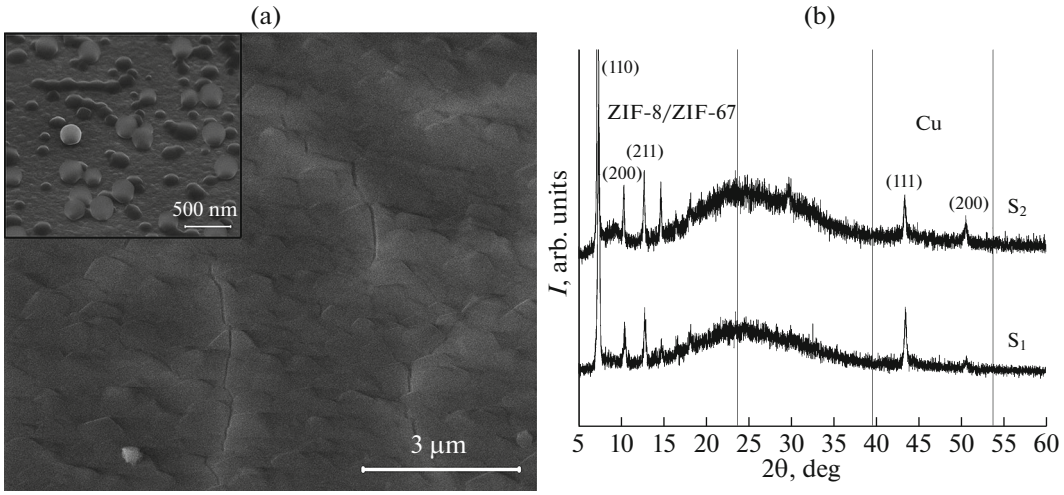

Fig. 3. SEM images of the MOF film after five deposition cycles (a) (in the inset, after the first cycle) and XRD spectra for the MOF films (b) in prototypes S_1 and S_2.

RESULTS AND DISCUSSION

Analysis of the obtained SEM images showed (Fig. 3a) that one deposition cycle leads to the formation of individual MOF crystals, and at least five deposition cycles are required to form a homogeneous film. According to the XRD data (Fig. 3b), it was established that the films in the S_1 prototype corresponds to ZIF-8 MOF. Reflections (110), (200), (211), and somewhat less intense ones in the range of 15°–20° correspond to the crystalline phase of ZIF-8 [16]. The diffraction profiles also show a broad peak in the range of 15°–40°, which indicates the presence of an amorphous phase of the quartz-glass substrate. Peaks characteristic of metallic-copper contact tracks are observed in the high-angle region.

Figure 3b shows the diffraction profile of the MOF film of prototype S_2, which confirms the preservation of the ZIF phase structure when zinc ions are replaced in the lattice by cobalt(II) ions.

As a result of measurements, it was established that at room temperature in an air atmosphere the resistance of the S_1 prototype film varies in the range of 1.2×10^5–4.5×10^8 Ω as the frequency increases from 20 Hz to 2 MHz (Fig. 4). Due to the fact that the resistance of metal electrodes does not depend on frequency, the observed decrease in the resistance of the sensitive element with increasing frequency (over 500 Hz) indicates the reactive nature of the resistance, which is typical for dielectric materials. A similar process was observed when changing the film capacity of the prototype S_1 in the low-frequency region (in the range of 30–110 Hz) with a maximum capacitance value of 20 pF (Fig. 4). A subsequent increase in frequency led to a decrease in capacitance, which indicates a weak inductive component, which is responsible for the increase in the capacitance of the structure with increasing frequency due to the compensation of capacitance reactance with inductive reactance. In addition, the capacitance can be affected by the structural elements of the sensor: its inductance and the resistance of the electrodes. The results obtained suggest a decrease in the dielectric constant of the ZIF-8 film due to the weakening of relaxation types of polarization and the absence of the influence of the inductive component. With a further increase in frequency to 1 kHz–2 MHz, the value of the dielectric constant barely changed, which may be due to the predominance of electronic and ionic polarization in the ZIF-8 film at these frequencies.

Studies concerning the temporal stability of the resistance and capacitance of the ZIF-8 film showed

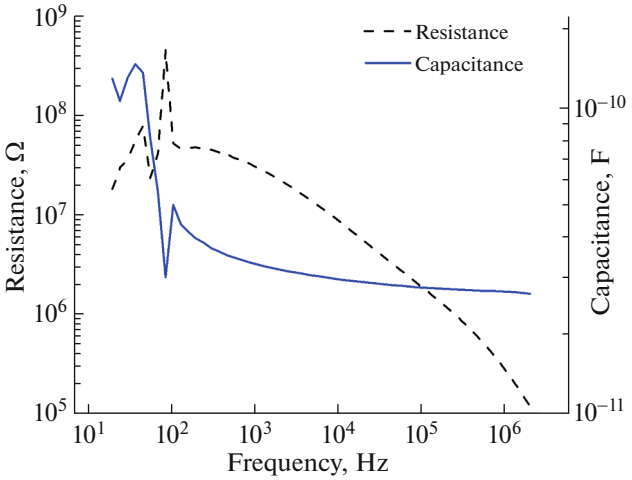

Fig. 4. Dependence of the resistance (dashed line) and capacitance (solid line) of prototype S_1 on the frequency of the signal.

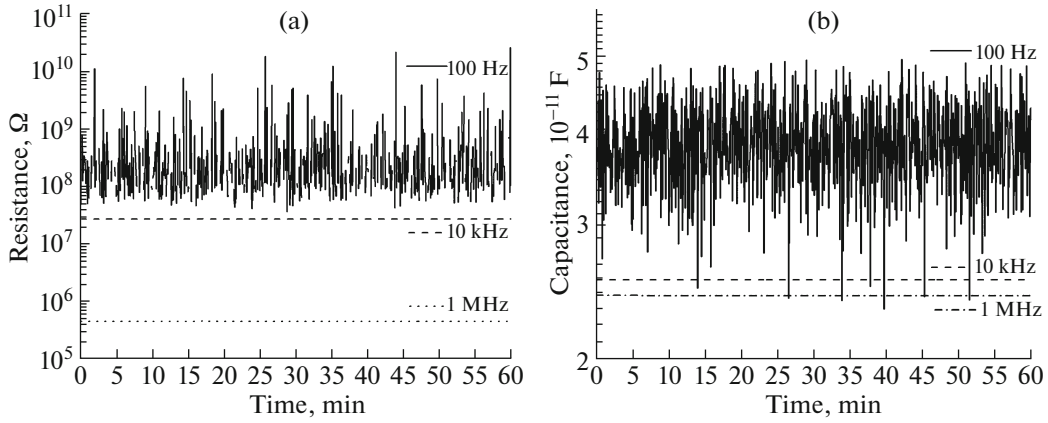

Fig. 5. Dependence of the temporal stability of the resistance (a) and capacitance (b) of the prototype S_1 at different frequencies.

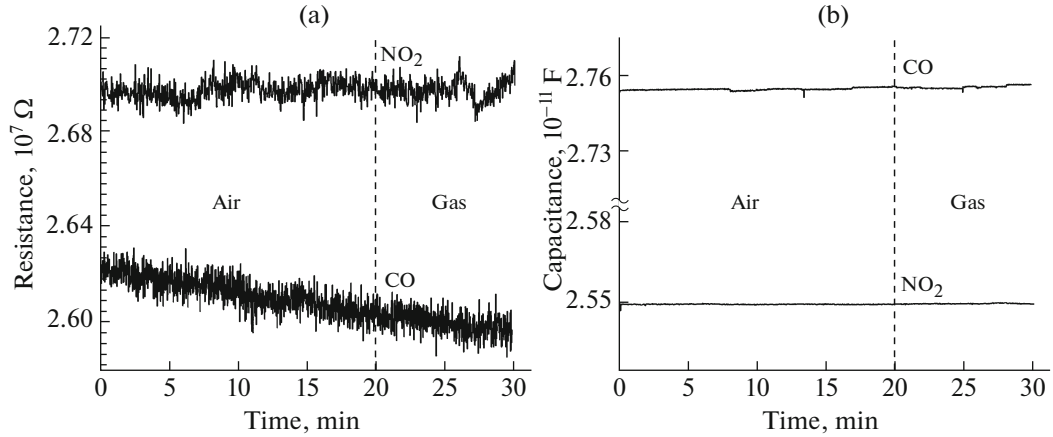

Fig. 6. Dependence of changes in the resistance (a) and capacitance (b) of the prototype S_1 when supplying target gases at room temperature.

high stability and a decrease in noise level with increasing measurement frequency (Fig. 5). In this case, a high noise level at low frequencies may indicate a high sensitivity of the sensitive element to external factors (atmospheric humidity, pressure, and temperature) affecting gas adsorption on the ZIF-8 film.

Studies of the ZIF-8 film for sensitivity to the target gases NO_2 and CO (275 and 30 ppm, respectively) did not show changes in the resistance (Fig. 6a) and capacitance (Fig. 6b) over the entire frequency range.

To increase sensitivity to the target gas NO_2, we conducted similar studies with heating of the S_1 prototype up to 150°C. As a result, it was found that the S_1 prototype is not sensitive to the supply of the target gas NO_2 at low concentrations (less than 45 ppm) and its resistance increases steadily without any clearly defined areas of peak changes (Fig. 7a). With increasing concentration of NO_2 up to 45 ppm, the sensor response was observed at all studied frequencies and showed a greater sensitivity at low measurement frequencies (1.9% for 100 Hz, 0.32% for 10 kHz, and 0.08% for 1 MHz). The maximum capacitive sensitivity was obtained at a frequency of 100 Hz (Fig. 7b), while its value was 2 times higher than the resistive sensitivity (Fig. 7a). Thus, for this sensor design, in order to reduce the influence of transient processes and increase the probability of detecting target gases at low concentrations, further experimental studies were carried out at a frequency of 100 Hz.

From the obtained dependences it was established that increasing the temperature allows an increase in the sensitivity of the sensor based on the ZIF-8 film when exposed to NO_2 as a result of the desorption of atmospheric moisture, freeing the pores of ZIF-8 for the adsorption of gases and reducing the activation energy. However, CO sensitivity was never found.

In order to detect CO and increase the probability of overcoming the energy barrier by reducing-gas molecules, as well as reduce the noise level during measurements, a prototype S_2 with the structure 3(ZIF-8) +

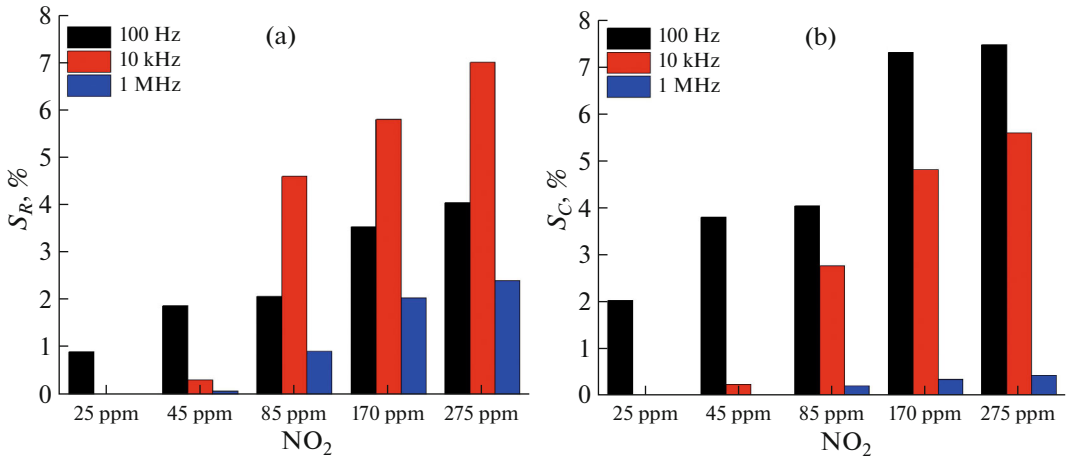

Fig. 7. Histogram of resistive (a) and capacitive (b) sensitivity of prototype S_1 depending on the measurement frequency.

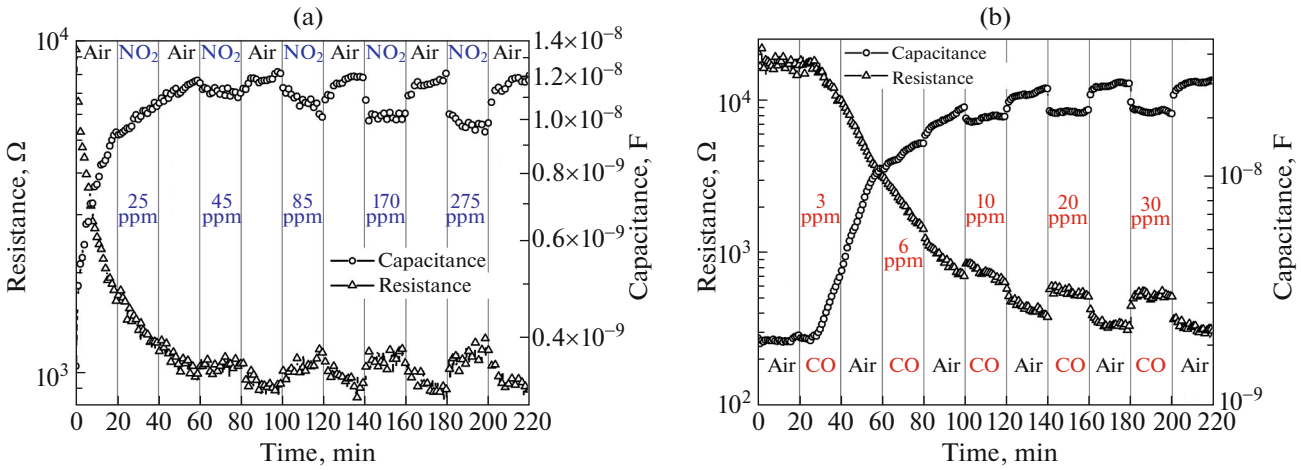

Fig. 8. Dependence of changes in the resistance and capacitance of the prototype S_2 when NO_2 (a) and CO (b) of different concentrations are supplied.

2(ZIF-67/ZIF-8) was fabricated. Studies of the response of the prototype S_2 to NO_2 and CO of different concentrations were carried out at a temperature of 180°C (Fig. 8).

The nonlinearity of changes in the capacitance and resistance of the prototype S_2 at the beginning of the process of supplying a gas with low concentrations of both CO and NO_2 (Fig. 8) may be associated with the gradual filling of the porous structure of the MOF with gas molecules, which leads to a decrease in resistance and an increase in the capacity of the film. In this case, the use of MOF films with the structure 3(ZIF-8) + 2(ZIF-67/ZIF-8) made it possible to initiate the sensitivity of S_2 to CO (Fig. 8b) and reduce the noise level during measurements. Based on the processing of the obtained data, histograms of the capacitive and resistive sensitivity of the S_2 prototype to the effects of NO_2 and CO of various concentrations were constructed (Fig. 9).

Figure 9a shows that with increasing NO_2 concentration from 45 to 275 ppm the resistive and capacitive sensitivity of the prototype S_2 increase from 3 to 19 and from 6 to 20%, respectively. A strong nonlinearity in changes in capacitance and resistance when NO_2 is supplied with a concentration of 25 ppm did not allow us to evaluate the sensor response for this gas concentration. The resistive and capacitive responses of prototype S_2 showed a high sensitivity to CO (Fig. 9b) even at low concentrations of 6 ppm (S_R = 9%, S_C = 7%) and 10 ppm (S_R = 15%, S_C = 10%).

Analysis of the responses of the prototypes S_1 (Fig. 7) and S_2 (Fig. 9) showed that the functionalization of ZIF-8 with two layers (ZIF-67/ZIF-8) leads to an increase in the sensitivity and response of the sensor S_2. This effect may be due to the fact that the

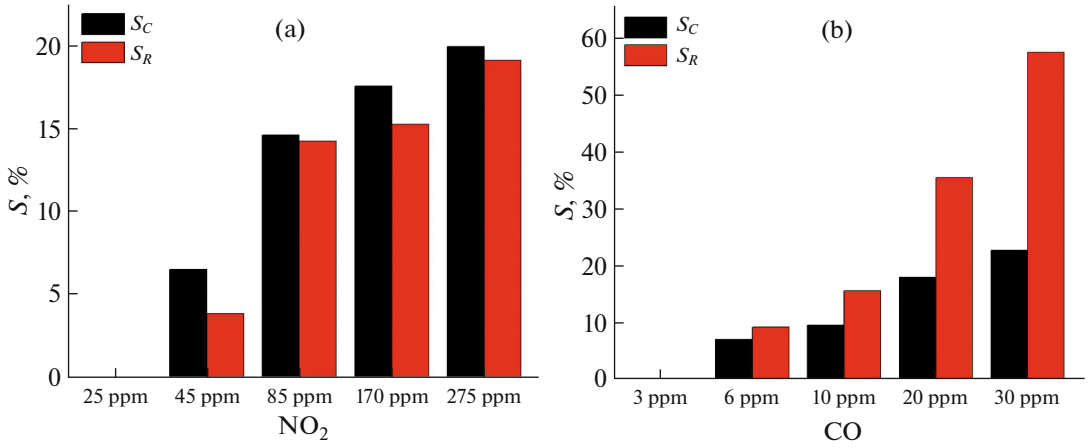

Fig. 9. Histograms of the capacitive and resistive sensitivity of the prototype S_2 to different NO_2 (a) and CO (b) concentrations.

cobalt(II) ion included in ZIF-67/ZIF-8 has the $3d^7$ electron level containing a vacant orbital along which the migration of electrons of target gases inside the *d* sublevel is possible. The zinc ion included in ZIF-8 has an outer electron layer of electron configuration $3d^{10}$, which means there is no vacancy *d* orbital. As a result, the conductivity of the prototype increases when using ZIF-67/ZIF-8. In addition, there is an increase in the impedance of the ZIF-67 layer due to the formation of additional capacitances, which affects the overall resistance of the structure and its response when gases are supplied. In this case, a gas of the same concentration causes different levels of capacitive and resistive response of the sensor.

CONCLUSIONS

The work implements a simple and cheap method for manufacturing gas sensors with a sensitive element based on MOF films. Heating the models promotes the desorption of atmospheric moisture, and also causes an increase in the capacity of the structure and a decrease in its resistance. It was shown that the functionalization of ZIF-8 films with layers of ZIF-67/ZIF-8 leads to an increase in the sensitivity of the sensor to NO_2 by more than 2 times compared to ZIF-8 films, and also allows CO detection. It has been established that for prototypes S_1 and S_2 a low measurement frequency (~100 Hz) makes it possible to reduce the influence of transient processes, and increase the relative sensitivity of measurements and the likelihood of detecting target gases of low concentrations. It was established that the considered MOF films react to NO_2 with a sensitivity of S_R = 3%, S_C = 6% (for 45 ppm) and S_R = 14%, S_C = 15% (for 85 ppm), and for CO even at low concentrations S_R = 9%, S_C = 7% (for 6 ppm) and S_R = 15%, S_C = 10% (for 10 ppm). It is shown that parallel analysis of the capacitive and resistive response makes it possible to increase the accuracy of the analysis of the sensor response when exposed to various gases and can be used as the basis for a software interface for training sensor operation using artificial intelligence.

ACKNOWLEDGMENTS

We are grateful to D.A. Khakhulin for help in automating the measurements.

FUNDING

The study was supported by the Russian Science Foundation (grant no. 22-29-01124) at the Southern Federal University, https://rscf.ru/project/22-29-01124/.

CONFLICT OF INTEREST

The authors of this work declare that they have no conflicts of interest.

REFERENCES

1. G. Hancke, B. Silva, and Jr. G. Hancke, Sensors **13**, 393 (2012). https://doi.org/10.3390/s130100393
2. S. Achmann, G. Hagen, J. Kita, et al., Sensors **23**, 8648 (2023). https://doi.org/10.3390/s23208648
3. S. K. Brown, M. R. Sim, M. J. Abramson, and C. N. Gray, Indoor Air **4**, 123 (1994). https://doi.org/10.1111/j.1600-0668.1994.t01-2-00007.x
4. R. A. Potyrailo, Chem. Rev. **116**, 11877 (2016). https://doi.org/10.1021/acs.chemrev.6b00187
5. P. Peterson, A. Aujla, K. Grant, et al., Sensors **17**, 1653 (2017). https://doi.org/10.3390/s17071653
6. A. Tricoli, M. Righettoni, and A. Teleki, Angew. Chem., Int. Ed. **49**, 7632 (2010). https://doi.org/10.1002/anie.200903801

7. T. Dutta, T. Noushin, S. Tabassum, and S. K. Mishra, Sensors **23**, 6849 (2023). https://doi.org/10.3390/s23156849
8. I. Stassen, N. Burtch, A. Talin, et al., Chem. Soc. Rev. **46**, 3185 (2017). https://doi.org/10.1039/C7CS00122C
9. H. Furukawa, K. E. Cordova, M. O'Keeffe, and O. M. Yaghi, Science **341**, 6149 (2013). https://doi.org/10.1126/science.1230444
10. O. M. Yaghi, M. O'Keeffe, N. W. Ockwig, et al., Nature **423**, 705 (2003). https://doi.org/10.1038/nature01650
11. S. Achmann, G. Hagen, J. Kita, et al., Sensors **9**, 1574 (2009). https://doi.org/10.3390/s90301574
12. Z. Hu, B. J. Deibert, and J. Li, Chem. Soc. Rev. **43**, 5815 (2014). https://doi.org/10.1039/C4CS00010B
13. L. E. Kreno, J. T. Hupp, and R. P. Van Duyne, Anal. Chem. **82**, 8042 (2010). https://doi.org/10.1021/ac102127p
14. V. Chernikova, O. Yassine, O. Shekhah, et al., J. Mater. Chem. A **6**, 5550 (2018). https://doi.org/10.1039/C7TA10538J
15. N. Jafari, S. Zeinali, and J. Shadmehr, J. Mater. Sci.: Mater. Electron. **30**, 12339 (2019). https://doi.org/10.1007/s10854-019-01592-7
16. K. S. Park, Z. Ni, A. P. Cote, et al., Proc. Natl. Acad. Sci. **103**, 10186 (2006). https://doi.org/10.1073/pnas.0602439103
17. A. M. Aboraia, A. A. Darwish, V. Polyakov, et al., Opt. Mater. (Amst.) **100**, 109648 (2020). https://doi.org/10.1016/j.optmat.2019.109648
18. S. Kempahanumakkagari, K. Vellingiri, A. Deep, et al., Coord. Chem. Rev. **357**, 105 (2018). https://doi.org/10.1016/j.ccr.2017.11.028